BEHAVIORAL MODELLING: VALIDATION AND INFORMATION THEORY CONSIDERATIONS

D. W. Repperger* and D. B. Rogers

Air Force Aerospace Medical Research Laboratory
Wright Patterson Air Force Base
Dayton, Ohio 45433, USA

W. N. Bianco

Systems Research Laboratory
Dayton, Ohio 45540, USA

Communicated by Xavier J. R. Avula

Abstract—A study is conducted on a behavioral model to study man–machine systems when exposed to physiological stress. Using such a model, an index related to human information processing is developed. By applying this model to empirical data from a centrifuge experiment, the index is calculated and shows some interesting results. By using such an index in conjunction with this model, the experimenter can develop a "design rule" on how to choose tracking performance tasks to further study different types of human tracking strategies.

1. INTRODUCTION

The behavior model concept [1] is an interesting approach in relating types of behavioral responses to a parametric representation of a model. If the model can classify different human responses into some parametric representation, then a variety of studies are possible. One could, for human experiments, vary an independent variable such as an environmental stressor and observe the changes in the empirical data resulting from the man–machine interaction. Once an accurate cause–effect relationship can be developed from the environmental stressor to human tracking performance, the model can then be used to predict changes in human behavior for a wide variety of different levels of the environmental stressor. This becomes an aid in the design of experiments to test protective equipment or other devices to enhance the human's tolerance to a stress environment. It is necessary in the design of these experiments to not only design the stress level to be of sufficient magnitude to incur a physiological stress on the subject but, in addition, it is necessary to design the tracking task to provide a mental workload requirement that is sufficiently challenging.

2. A DESCRIPTION OF THE MAN–MACHINE INTERACTION

Figure 1 illustrates a block diagram description of the man–machine experiment that will be considered in this paper. $f(t)$ is a variable which describes the target forcing function which
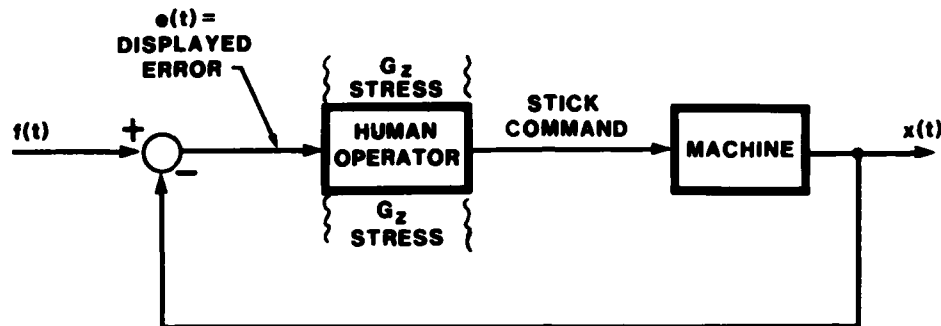
Fig. 1. Open-loop stress.

appears on a cathode ray oscilloscope. The human observes on the display the closed loop tracking error [dentoed here as $e(t)$] and makes stick commands which become the input into a block labeled "machine." The output of the machine is the variable $x(t)$ which is compared to the reference trajectory $f(t)$ resulting in the error $e(t)$ being the difference between $f(t)$ and $x(t)$. As the human makes stick commands, these inputs drive the cab roll dynamics of a 3 degree-of-freedom simulator (centrifuge) which induces an acceleration stress denoted as $+ Gz$. The term Gz means an acceleration stress vector pointing down the spine of a subject. The acceleration stress levels created by the centrifuge produce physiological discomfort. Under this effect the subject reduces the levels of his stick commands and does not attempt to track the target $f(t)$ with the accuracy he has under the no stress condition. In th.s sense the subject trades off "pain to performance."

3. THE BEHAVIORAL MODEL

An important aspect of human tracking involves behavior changes [2]. Studies of human tracking indicate that behavior modifications [which are manifested by dramatic changes in characteristics of the tracking error $e(t)$] can also be due to properties of the task variable $f(t)$. This is best illustrated in Fig. 2 in which a dichotomy of behavior can now be explicitly stated.

In Fig. 2, the variable f denotes the velocity (time rate of change of position) of the task variable $f(t)$. f denotes the acceleration of $f(t)$ with respect to time. From previous studies on human tracking it has been determined that for small values of f and f (corresponding to behavior region I inside the circle), the tracking task is easy to follow and the subject maintains high levels of accuracy in tracking. If, however, the trajectory $f(t)$ gets outside a critical boundary (and enters into region II—the difficult tracking region), a behavior change is known to occur. The target variable $f(t)$ has excessively large values of velocity and acceleration in region II, which results in the human exhibiting "regressive behavior." The term regressive behavior is borrowed from the psychological literature which means that the subject will substantially reduce his stick commands and not try to track the target. It is to his benefit (in a performance sense) to exhibit this type of behavior because in region II, increasing stick commands only result in larger error signals.

Thus it is seen that human tracking behavior defined in this context is influenced by the following two variables:

(1) Physiological stress—In this case the human will trade off tracking performance to discomfort induced by the environment.

(2) Characteristics of $f(t)$—If the task moves too quickly, regressive behavior is known to occur.
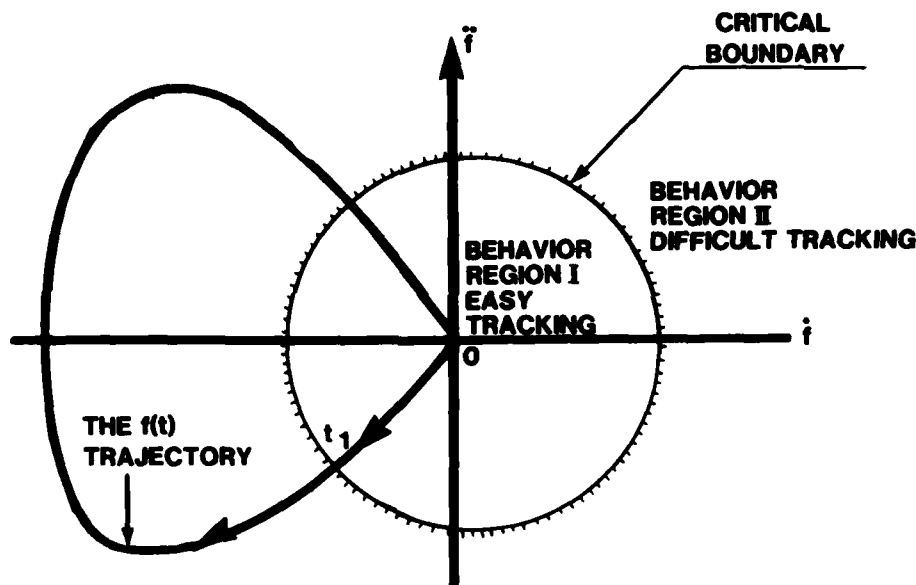
Fig. 2. The behavior regions.

It is desired to incorporate both of these concepts into a behavior type model. To achieve this result, Fig. 2 illustrates this concept. The behavior model assumes the following:

(1) A critical boundary exists which separates region I from region II. For simplicity, this boundary will be assumed to be characterized by a circle.

(2) Inside this boundary defines region I, an easy tracking region represented by small absolute values of f and $\dot{f}$ (inside the circle).

(3) Outside this boundary defines region II, where the human behavior is characterized by regressive responses. This is assumed to correspond to large values of $|f|$ and/or $|\dot{f}|$.

(4) All human tracking behavior is divided into only two regions. This assumption seems tenable based on discussions with pilots involved in air combat situations in which aircraft try to out maneuver each other.

(5) The critical boundary shrinks or expands under the following conditions:

(a) For severe levels of environmental stress, the boundary will shrink. This indicates a smaller capable region of tracking.

(b) The addition of assistive devices (e.g., a lead angle computer for a gun system) may increase the size of the boundary. This has been shown to be the case in certain gun systems [3].

(c) A good tracker will have a larger tracking capability region as compared to a poor tracker. This has also been shown empirically [2].

4. A STATISTICAL ALGORITHM TO VALIDATE THE BOUNDARIES

The one element remaining in this type of model is a decision rule to describe in some manner the critical boundary. In Fig. 3, a plot of $\dot{e}(t)$ versus $e(t)$ is constructed using similar arguments as described previously [2]. Region I can be assumed to be within an elliptical area; region II will appear outside this area. It is also shown in the appendix that the variable $e(t)$ is actually a stochastic process $e(t, x)$ but is denoted here in the text of this paper as $e(t)$.
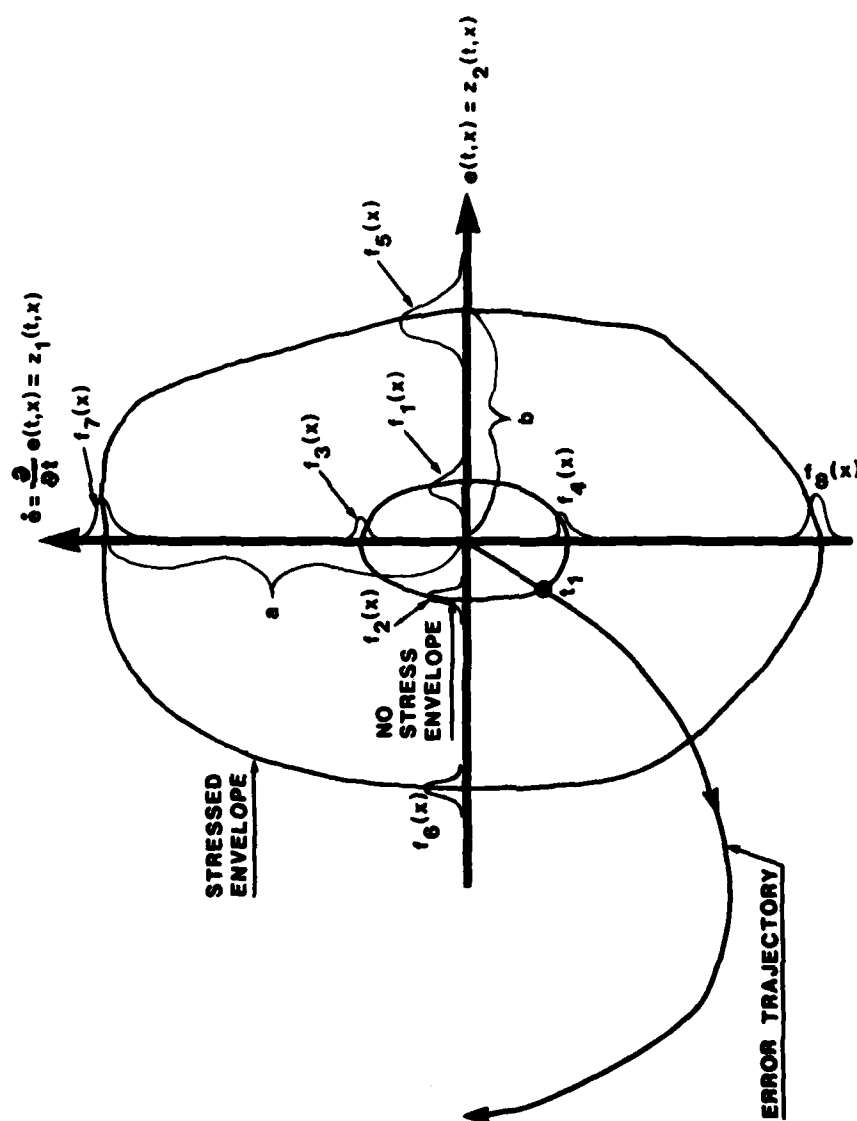
Fig. 3. The phase plane representation with and without stress.

The distribution functions $f_1(x)$ and $f_3(x)$ which characterize this phase plane boundary in Fig. 3 are interrelated by a correlation relationship. This is discussed in more detail in the appendix.

In Fig. 4, the statistical decision rule from [2] is illustrated in a heuristic manner. Data values obtained from either $|e|$ or $|\dot{e}|$ are plotted versus time. During the region I types of behavior, the dependent variable ($|e|$ or $|\dot{e}|$) has a value close to α. This corresponds to the axis of the variable of interest in the ellipse in Fig. 3. At the time t_1 (cf. Figs. 3 and 4), the value of this variable changes from approximately α to β units. The dependent variable must maintain a level of β units for at least t_2 sec to be considered into region II. The statistical decision rule depends on the relative values of β and α and is, in itself, a random variable. Thus there may be some error in defining the critical boundary (it is not deterministic), but this error can be obtained from the properties of the distribution functions $f_1(x)$ and $f_3(x)$.

5. LINKS TO INFORMATION THEORY

It is desired in this paper to relate the model thus described in such a manner analogous to an information theoretic method. The calculation of channel capacity in information theory is no simple task. Such a calculation depends on properties of the input and output signals, the noise processes, and the type of channel considered (continuous or discrete). For the special case of a bandlimited input signal with bandwidth W (rad/sec), and a time continuous Gaussian channel [4], the capacity of such a channel can be written

$$C_p = W \ \log(1 + S/N),\qquad(1)$$

where S and N are, respectively, the signal power and the noise power in the channel. The quantity C_p (units of bits/sec) in Eq. (1) provides a useful bound in determining actual transmission rates in a channel and also in calculating capacities for other types of channels (e.g., a time-discrete Gaussian channel). It can be shown [4] that C_p provides an upper bound for all transmission rates in a channel.
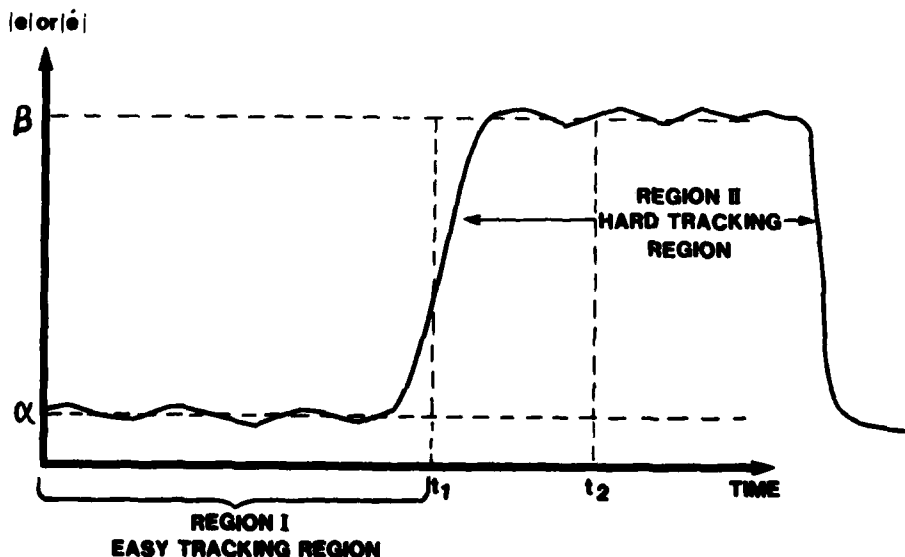

Fig. 4. The statistical decision rule.

The variable of interest in Eq. (1) is the ratio (S/N). In the field of communications, the figure of merit (S/N) describes the important aspect of a channel in detail. For example, if (S/N) is 10 or greater, it is generally accepted as a good channel for transmission of information. In an analogous manner, variables similar to (S/N) find application in the fields of psychophysics under differerent labels. For example, in the area of manual control, tracking experiments have shown for hand control studies what is referred to as a Weber's law effect. If N_x represents the signal power in the hand control activity not correlated to a tracking task and S_x represents the total signal power, the ratio

$$20 \log_{10}(N_x/S_x) = -20 \, dB \qquad (2)$$

is a well known relationship determined from remnant studies [5, 6] which holds for the low frequency range where most of the control (stick power) is known to occur. The relationship from Eq. (2) implies that

$$S_x/N_x \approx 10 \qquad (3)$$

holds for normal neuromotor tremor response in this type of situation. A similar type of effect is known to occur in situations involving the lifting of a weight. If a human were to lift a weight of W_1 pounds above his head, and if ΔW_1 was the root mean square measure of the variability (or tremor) associated with this weight, then the ratio

$$(\Delta W_i)/W_i = \text{constant} \qquad (4)$$

is known to hold for a wide range of W_i values up to a maximum. This is sometimes referred to as the "Henneman's Size Principle" and implies that variability increases in proportion to the disturbing force. Thus, for larger weights, one sees larger variability, as is expected.

A fourth area where this type of information theoretic concept occurs is in parameter identification procedures. If μ denotes an estimate of a parameter and σ its variance in this estimate, the ratio

$$I = \sigma/\mu \qquad (5)$$

becomes a valid indication of system order [7]. When I is minimized with respect to the unknown parameters σ and μ, the system's order can be determined. A rigorous test on system order can be made using this type of index. If I exhibits values less than 0.1, the order of a system can be determined within accepted scientific levels ($p < 0.05$). An interesting discussion on the use of invariant constants can be found in the classical paper [8] by Miller related to distinguishing a variety of psychophysical stimulus. Discussions in [9, 10] also provide motivation for studies of this type although it has been known [11] that information theoretic models of humans involved in tracking tasks have not found wide application.

The ability of humans to act like information channels yields some provocative results. If capacity is measured in units of bits/sec, studies related to a wide number of reading experiments yield [14] rates on the order of 40–50 bits/sec for this type of information channel. In terms of vision, however, Kelly [15] measured the information capacity of a single human retina and obtained a figure of 10^9 bits/sec. This number seems high compared to recent measurements of visual capacity [16] which indicate a minimum of 50,000 bits/sec as the required amount of visual information necessary to discriminate pictures for undersea work.

The measurement of capacity as bits/sec should not be confused with the classical work by Miller [8] which is concerned with capacity using units of bits/judgment. Miller's law showed that the number of categories for which simple objects of a one dimensional stimulus

could be assigned to is consistently near 7 ± 2 for a wide range of different tasks. This means approximately 3 bits/judgment is the capacity of a human for a one-dimensional stimulus. Sheridan [11] clearly explains that the human sensors act in a multitude of dimensions (each dimension of which can only distinguish 7 shades of stimulus). Therefore the high capacity rates associated with the reading of words and the visual information channel are due to the fact that these sensors are composed of a multidimensional channel, each dimension having capacity limited by 3 bits/judgment.

These works also support the concept that when working at capacity, one can increase speed only at the expense of accuracy, and conversely. For example in the study of motor acquisition tasks, Fitts' law [17] concurs with the capacity measure of 2–3 bits/judgment (7 alternatives) and recent work [18] supports this fact in the modern laboratory environment. It is, therefore, desired in this study to use a variable of the form I in Eq. (5) related to the behavior model discussed previously to exhibit invariance properties that occur in information theoretic models, as has been discussed here.

6. APPLICATIONS TO A BEHAVIOR MODEL

In order to apply the previous concepts to the behavior model developed in the last section, it is necessary to define a useful metric related to tracking performance behavior. If the variable representing the performance is a good measure, one would expect ratios of (variations in intensity/mean intensity) to show some consistency over various levels of stress.

To achieve this goal, it is first necessary to define the measure of variability (mean $\hat{\mu}$ and standard deviation $\hat{\sigma}$). Figure 3 illustrates the diagram that will be used in this procedure. A plot is made of the time derivative of $e(t)$ versus $e(t)$. The densities $f_i(x)$, $i = 1, 2 \ldots 8$, in Fig. 3 are determined through averages across replications of the experiment and their structures are not specified at this point in time. It is necessary to first define the boundaries of the $\dot{e}(t)$ and $e(t)$ axis.

Definition. The phase plane boundary $= \hat{\mu}_i$, where

$$F_i(\hat{\mu}_i) = 0.5, \quad i = 1, 2 \ldots 8 \tag{6}$$

and $F_i(x)$ satisfies

$$F_i(x) = \int_{-\infty}^{x} f_i(s) \, ds, \tag{7}$$

$i = 1, 2 \ldots 8$ and $f_i(s)$ is the appropriate density function. Thus, the boundaries of the phase plane are defined with respect to median values which can be related to those obtained from the empirical data (even if the underlying densities are unknown). To determine the ± 1 S.D. envelopes about the means, data are averaged across replications in the following manner:

(1) Find the maximum window (across all replications $k = 1, 2 \ldots j$).
(2) Divide all windows up into 20 equal parts using $0, x_1, x_2 \ldots x_{20}$.
(3) At each x_i, find the $F_i(x_i)$ value across the j replications that corresponds to this value of x_i.
(4) Then average the F_j as follows:

$$F_j = \sum_{k=1}^{j} (F_k) = \text{mean} \tag{8}$$

$$\hat{\sigma}_{F_j} = \sum_{k=1}^{j} [(F_k - F_j)^2 / j]^{(1/2)} = \text{S.D.} \tag{9}$$

The next step in this procedure is to develop a parametric ratio which can be used to study properties of the human as an information processor. This index should be tested for consistency and satisfy properties similar to the other variables discussed. The index chosen here is specified by

$$I = \hat{\sigma}_{F_j}/\hat{\mu},$$ (10)

where $\hat{\sigma}_{F_j}$ satisfies Eq. (9) and $\hat{\mu}$ is specified by (6).

7. EMPIRICAL VALIDATION OF THIS INDEX

Two tests will be conducted on the variable I specified in Eq. (10). First, a test on consistency across experimental conditions will be performed (analogous to Weber's law). Second, the calculation of processing bandwidth will be conducted for two experimental conditions.

The data base used in this paper covers an interesting experiment in the area of acceleration stress [12]. As described earlier in Sec. 2, human subjects were exposed to acceleration forces while simultaneously required to perform a tracking task. Figure 5 illustrates the stress levels and durations of exposure. Five different tasks were chosen in this study based on different levels of velocity and acceleration profiles of the variable $f(t)$. A more complete description of the experiment can be found in [12]. For simplicity only the analysis details related to information theory are considered here.

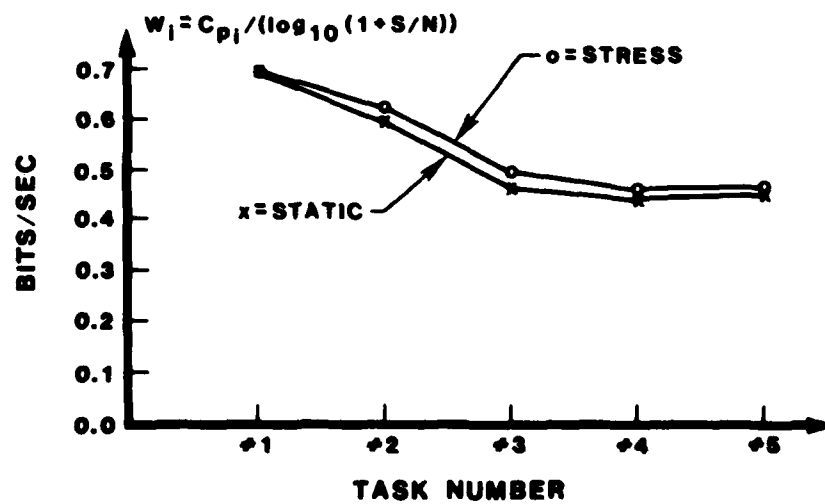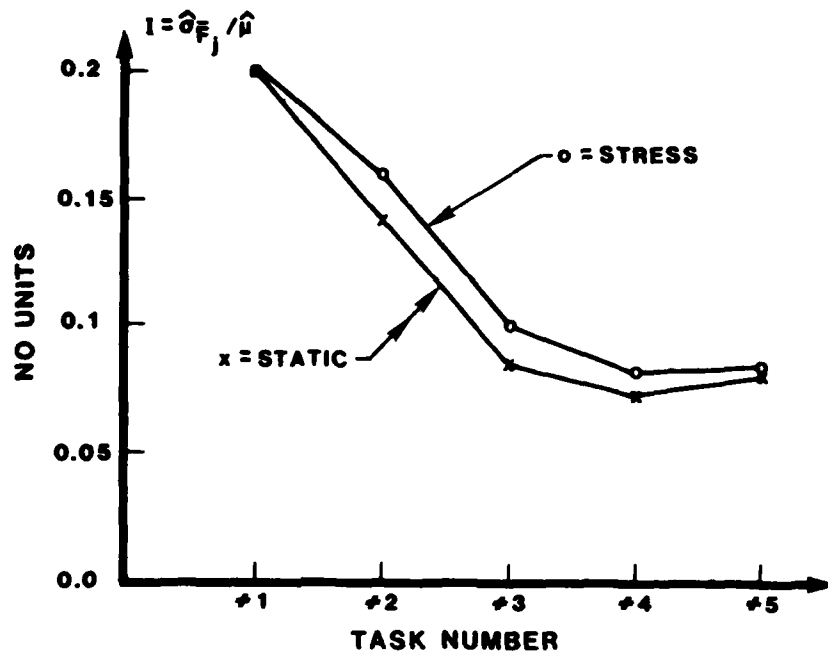The first test of interest in these data is the level of consistency of the variable I in Eq.

Fig. 5. A temporal description of the G stress exposure.
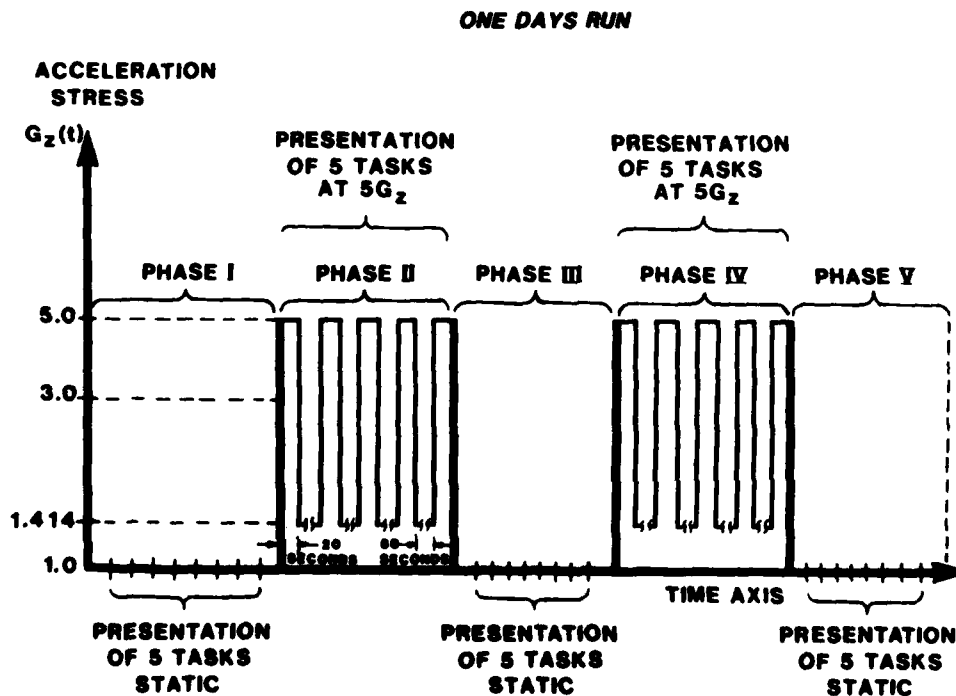
Fig. 6. (Top) I versus task number; (Bottom) W_i versus task number.

Table 1. Values of I (7 subjects 4 replications).

Exp. Cond.	ff ≠ 1			ff ≠ 2			ff ≠ 3			ff ≠ 4			ff ≠ 5		
	$\hat{\mu}$	$\hat{\sigma}$	I	$\hat{\mu}$	$\hat{\sigma}$	I	$\hat{\mu}$	$\hat{\sigma}$	I	$\hat{\mu}$	$\hat{\sigma}$	I	$\hat{\mu}$	$\hat{\sigma}$	I
Static	0.45	0.09	0.2	0.70	0.1	0.143	1.2	0.10	0.083	1.5	0.11	0.073	1.6	0.13	0.081
Stress	0.55	0.11	0.2	0.75	0.12	0.16	1.3	0.13	0.1	1.7	0.14	0.082	1.8	0.15	0.083

(10). If, indeed, this variable is a viable measure of human tracking, one would expect a Weber's law effect to hold. Using data from 7 subjects, 4 replications of each experimental condition, Table 1 is constructed.

From Table 1 it is seen that as the task number increases, the variability ($\hat{\sigma}$) increases. Also, going down a column, both $\hat{\mu}$ and $\hat{\sigma}$ increase. This is typical of data from a stress experiment of this type. The ratio $\hat{\sigma}/\hat{\mu}$, however, does not show consistency going across a row in either the stress or static condition.

A second calculation is conducted which involves processing bandwidth using the values of C_p specified in Eq. (1). If the capacity of the human is constant, one could write the processing bandwidth in the following form:

$$W_i = C_{p_i}/[\log_{10}(1 + S/N)], \tag{11}$$

where i stands for stress or static. The variable $(1 + S/N)$, related to units of $[1 + (1/I)^2]$, is calculated and illustrated in Table 2 with W_i in units of C_p and let

$$a = [1 + (1/I)^2]. \tag{12}$$

The data displayed in Tables 1 and 2 are illustrated in Figs. 6a-b. Table 2 illustrates some important results. For tasks 1 and 2 (ff ≠ 1 and ff ≠ 2), there appears to be high levels of W_i. For tasks 3, 4, and 5 a different set of the W_i values appear. This seems to indicate that this experiment produces two types of tracking behavior (both occurring in region I of tracking). The high accuracy tracking occurred for tasks 1 and 2. For the remaining 3 tasks, a different type of tracking behavior is noted.

One hypothesis to explain these results found in the data comes from studies in muscular activity. Physiologists speak of slow twitch muscles and fast twitch muscles when describing arm movements in tracking. The data seem to reflect this type of effect. The slow twitch muscles are used for the accurate tracking in tasks 1 and 2. The fast twitch muscles are used in tracking where large amounts of force are required. Since this experiment used control sticks that had large force gradients for the higher numbered tasks, this model indicates a transition between the two types of muscle activity between tasks 2 and 3. Thus, the modelling gives us a clue as to how to design these tasks to investigate which type of muscle activity

Table 2. W_i in terms of C_p units and a.

Exp. Cond.	ff ≠ 1		ff ≠ 2		ff ≠ 3		ff ≠ 4		ff ≠ 5	
	a	W_i	a	W_i	a	W_i	a	W_i	a	W_i
Static	26	0.707	49.9	0.592	145	0.490	187	0.440	153	0.458
Stress	26	0.707	40.06	0.624	101	0.498	148	0.461	145	0.463

is affected by the acceleration stress. Therefore by noting the task numbers producing different types of tracking responses, we can design tasks necessary to study this effect.

8. SUMMARY AND CONCLUSIONS

This study discusses a behavioral model which incorporates physiological stress and task variables. Some similarities are noted between data from this model and information theory. A proposed index for measuring human information processing properties in the behavioral model was tested for consistency and the processing bandwidth was calculated for two experimental conditions. Phase plane analysis provided insight into different types of tracking which can be used to further investigate how humans use muscle activity in hand control. By using the behaviorial model and analyzing the data, the experimenter developed a *modus operandi* as to how to design the tracking tasks for the next experiment to study different aspects of human tracking. Thus the use of a mathematical model increased our knowledge about the underlying physical process occurring in the data.

APPENDIX A

In this appendix the closed loop error signal denoted as $e(t)$ in the text is analyzed here as a stochastic process $e(t, x)$, where x is the distribution of the window variable and t is the time evolution of the error signal. Thus, with reference to Fig. 3, if the closed loop error signal (no stress) crosses the positive $e(t)$ axis at time instant t_1, time can be frozen at t_1 units and the random variable $f_1(x)$ becomes the window distribution at that point in time, i.e.,

$$f_1(x) = e(t_1, x). \tag{A.1}$$

Likewise, if the closed loop error signal crosses the positive $\dot{e}(t)$ axis at time t_2, the random variable $f_3(x)$ is likewise specified by

$$f_3(x) = (\partial/\partial t)e(t, x)|_{t=t_2}. \tag{A.2}$$

To illustrate the difference in the vertical and horizontal axis in Fig. 3, the variable $z_1(t, x)$ will denote the vertical axis and $z_2(t, x)$ will denote the horizontal axis. Thus,

$$z_1(t, x) = (\partial/\partial t)e(t, x) \tag{A.3a}$$

$$z_2(t, x) = e(t, x) \tag{A.3b}$$

In this appendix, the assumptions governing the phase plane boundaries will be discussed in detail. With reference to Fig. 3, the following assumptions will be considered.

Symmetry Assumptions

(B.1) $f_1(x)$ and $f_2(x)$ are of similar structure and symmetrical about their medians, i.e.,

$$f_1(\mu_1) = f_2(-\mu_1) \tag{A.4}$$

In a similar manner, this property is assumed to apply to $f_5(x)$ and $f_6(x)$.

(B.2) $f_3(x)$ and $f_4(x)$ are of similar structure and symmetrical about their medians, i.e.,

$$f_3(\mu_2) = f_4(-\mu_2). \tag{A.5}$$

Similarly, this property is assumed to apply to $f_7(x)$ and $f_8(x)$.

Assumptions governing the ellipse

(B.3) $f_3(y)$ is unknown, but $f_3(y)$ may not be of the form $f_1(x)$, i.e.,

$$f_3(y) \neq f_1(x) \tag{A.6}$$

where $y = cx + d$ is a linear relationship and c and d are constants.

(B.4) The time evolution of the elliptical path is governed by

$$(z_1)^2/a^2 + (z_2)^2/b^2 = 1 . \tag{A.7}$$

(B.5) In the phase plane, the following dynamical equation holds:

$$(\partial/\partial t)z_2(t, x) = z_1(t, x) \tag{A.8}$$

(B.6a) $f_i(x)$, $i = 1, 2$ are normal,
(B.6b) $f_i(x)$, $i = 3, 4$ are normal.

This appendix will examine the feasibility of assumptions (B.1)–(B.6) and derive properties arising from these conditions. It will first be necessary to show the following interrelationships between these assumptions.

Lemma 1. (B.6a) and (B.4) together imply (B.6b) is false.

Proof. Solving (A.7) for z_2 yields

$$z_2 = \sqrt{b^2 - (b/a)^2 z_1^2} . \tag{A.9}$$

If z_2 has density $f_1(x)$ associated with this axis, then the density of z_1 subject to (A.9) can be determined by coordinate transformation [13]:

$$f_3(y) = f_1[(b^2 - (b/a)^2 z_1^2)^{(1/2)}](\partial/\partial z_1)[(b^2 - (b/a)^2 z_1^2)^{(1/2)}]\big|_{z_1 = y} \tag{A.10}$$

or

$$f_3(y) = (b^2/(\sqrt{2\pi}a^2\sigma)(y/(b^2 - (b/a)^2 y^2)^{(1/2)}) e^{((b^2 - (b/a)^2 y^2)^{(1/2)} - \mu)^2/2\sigma^2)} \tag{A.11}$$

If one now attempts to write this in the form

$$f_3(y) = K[1/(\sqrt{2\pi}\sigma_y) e^{-(y - \mu_y)^2/2\sigma_y^2}] , \tag{A.12}$$

where y is a linear function of the variable x, one sees this cannot be done due to the term $y/(b^2 - (b/a)^2 y)^{(1/2)}$ in (A.11). Thus the density $f_3(y)$ derived by assumptions (B.6a) and (B.4) imply that (B.6b) is not satisfied. Next, assumptions (B.4) and (B.5) will be examined to see if they give rise to some level of consistency.

Lemma 2. The assumptions (B.4) and (B.5) are consistent with $f_1(x)$ arbitrary and $f_3(x)$ satisfying (A.10).

Proof. Combining Eqs. (A.7) and (A.8) yields

$$(\partial/\partial t)z_2(t, x) = \sqrt{a^2 - (a/b)^2 z_2^2}\big|_{x = \text{constant}} \tag{A.13}$$

or

$$dz_2/(\sqrt{a^2 - (a/b)^2 z_2^2}) = dt \qquad\qquad (A.14)$$

becomes the first integral

$$(b/a)(\sin^{-1}(z_2/b)) = t - t_0 \qquad\qquad (A.15)$$

or

$$z_2(t, \mu_2) = b \sin(a(t - t_0)/b) \qquad\qquad (A.16)$$

and $z_1(t, \mu_1)$ becomes, from (A.7),

$$z_1(t, \mu_1) = a \cos(a(t - t_0)/b) . \qquad\qquad (A.17)$$

Thus the stochastic process may evolve in time via the parametric elliptical equations (A.16-17). It is noted at this point that the density functions $f_1(x)$ and $f_3(y)$ are still arbitrary. From the derivation in Lemma 1, however, it is noted that if $f_1(x)$ is specified, then $f_3(y)$ has a dependence through the coordinate transformation [Eq. (A.10)].

In summary, the following assumptions concerning the stochastic process $e(t, x)$ can be stated which are consistent with all the analysis conducted in this paper:

(I) In the phase plane axis, the following relationship holds for all x:

$$(\partial/\partial t)(e(t, x)) = (\partial/\partial t)z_2(t, x) = z_1(t, x) . \qquad\qquad (A.18)$$

(II) The time evolution of the elliptical path is governed by

$$(z_1^2)/(a^2) + (z_2^2)/(b^2) = 1 . \qquad\qquad (A.19)$$

(III) The density of $f_1(x)$ may be specified. From [12] it is known that this function should not be assumed to be normal. If $f_1(x)$ is specified then the density $f_3(y)$ must satisfy

$$f_3(y) = f_1(\sqrt{(b^2 - (b/a)^2 z_1^2)}) \cdot (\partial/\partial z_1) \cdot [((b^2 - (b/a)^2 z_1^2)^{(1/2)})]|_{z_1 = y}|_{t = \text{specified}}. \qquad (A.20)$$

REFERENCES

1. T. Nishikawa, Analysis of the behavioral system by using control theory, in Proceedings of the First International Conference on Mathematical Modeling, Institute for Applied Sciences, St. Louis, Missouri 1977.
2. D. Repperger, S. L. Ward, E. J. Hartzell, B. C. Glass, and W. C. Summers, An algorithm to ascertain critical regions of human tracking ability. *IEEE Trans. Systems, Man, Cybernet.* SMC-9, 183–196 (1979).
3. D. Repperger and M. M. Vikmanis, Analysis of a tracer fire system as a man–machine problem, in Proceedings of the 15th Annual Conference on Manual Control. AFFDL-TR-79-3134 (1979).
4. R. Ash, *Information Theory*, Interscience, New York (1967).
5. W. H. Levison, S. Baron, and D. L. Kleinman, A model for human controller remnant. *IEEE Trans. Man-Machine Systems* MMS-10, 101–108 (1969).
6. H. R. Jex, R. W. Allen, and R. E. Magdaleno, Display format effects on precision tracking performance, describing functions, and remnant. AMRL-TR-71-63 (1971).
7. V. K. Desai and F. W. Fairman, On determining the order of a linear system. *Math. Biosci.* 12, 217–224 (1971).
8. G. A. Miller, The magical number seven, plus or minus two: Some limits on our capacity for processing information. *Psycholog. Rev.* 63, 81–97 (1956).
9. W. R. Garner and William J. McGill, The relation between information and variance analysis. *Psychometrika* 21, 219–228 (1956).

10. E. Crossman, The information-capacity of the human motor system in pursuit tracking. *Q. J. Exp. Psychol.* **XII**, 1–16 (1960).
11. T. B. Sheridan and W. R. Ferrel, *Man–Machine Systems Information, Control and Decision Models of Human Performance*, MIT Press, Boston (1974).
12. D. Repperger and D. B. Rogers, A task difficulty G stress experiment (submitted for publication).
13. R. V. Hogg and A. T. Craid, *Introduction to Mathematical Statistics*, 4th Ed., 132–143, MacMillan, New York (1978).
14. J. R. Pierce and J. E. Karlin, Reading rates and the information rate of a human channel. *Bell System Tech. J.*, **1957**, 497–516.
15. D. H. Kelly, Information capacity of a single retinal channel, *IRE Trans. Information Theory* IT-8(3), 221–226 (1962).
16. T. B. Sheridan and V. Ranadize, Video framerate, resolution, and grayscale tradeoffs for undersea telemanipulator control, 17th Annual Conference on Manual Control (1981).
17. P. M. Fitts, The information capacity of the human motor system in controlling the amplitude of movement. *J. Exp. Psychol.* **47**, No. 6 (1954).
18. R. J. Jagacinski, D. W. Repperger, S. L. Ward, and M. S. Moran, A test of Fitts' law with moving targets. *Human Factors* **22**, 225–233 (1980).